UNIVERSITÀ DEGLI STUDI DI PADOVA

Dept. of Civil, Environmental and Architectural Engineering

Numerical Modeling of Fault Activation and Induced Seismicity in Gas Storage Reservoirs: The Netherlands Case

Massimiliano Ferronato, Andrea Franceschini, Carlo Janna, Pietro Teatini, Claudia Zoccarato

SIAM Conference on Mathematical and Computational Issues in the Geosciences (GS19)

March 11-14, 2019 – Houston, TX

Outline

- Introduction: geohazards associated with Underground Gas Storage (UGS) activities
- The Netherlands case: conceptual model for the inception of fault movements
- Mathematical and numerical model: numerical discretization of fault mechanics by Lagrange multipliers
- Numerical results: factors that can enhance the probability of fault reactivation
- Conclusions: preliminary practical indications

- The interest in developing UGS projects is continuously increasing worldwide
  - May 2015: over 270 plants in Europe, 400 in the US
- Geohazards associated with UGS activities:
  - Formation integrity
  - Leakage from the reservoir
  - Land motion
  - Induced and/or triggered seismic events
- Coping with such issues is necessary for health and safety as related to public perception, economic risk and environmental impact

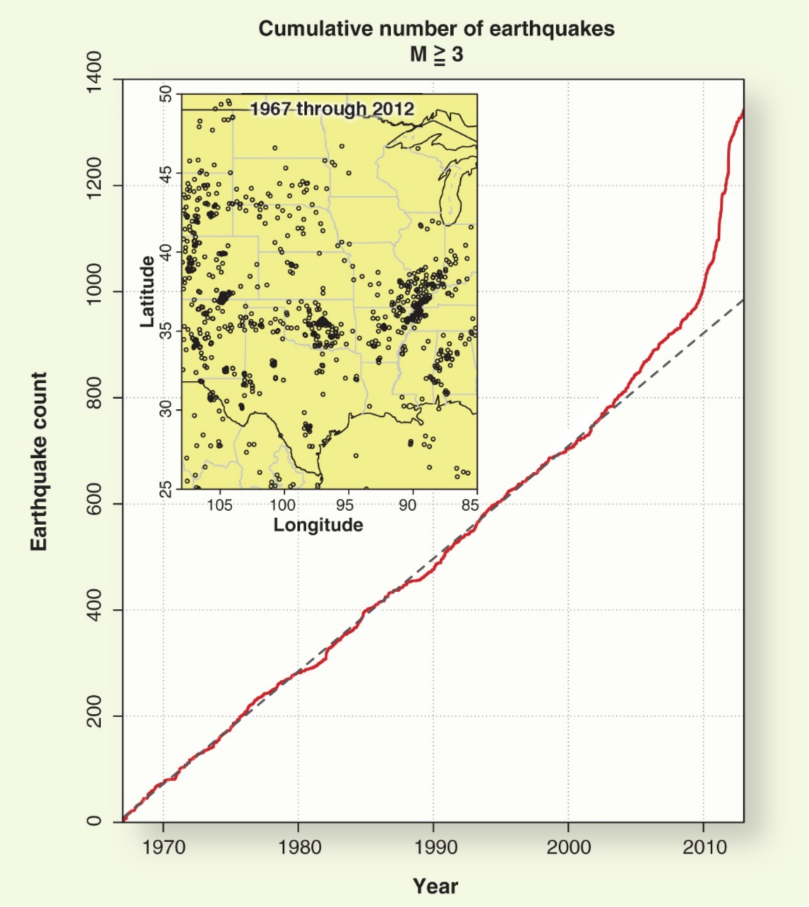

from Ellsworth (Science, 2013)

- Cases of seismic activity have been recently recorded in a few UGS plants in the Netherlands
  - Primary Production
  - Cushion Gas injection
  - Storage activities
- Highly compartmentalized and fractured reservoirs in stiff rocks overlain by salt deposits

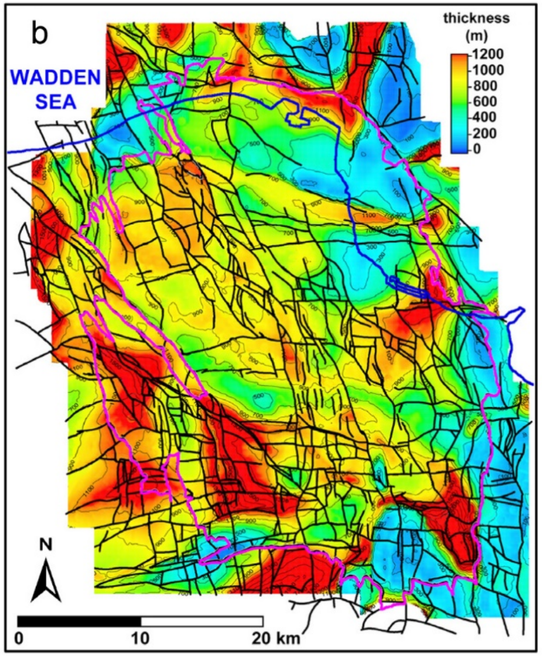

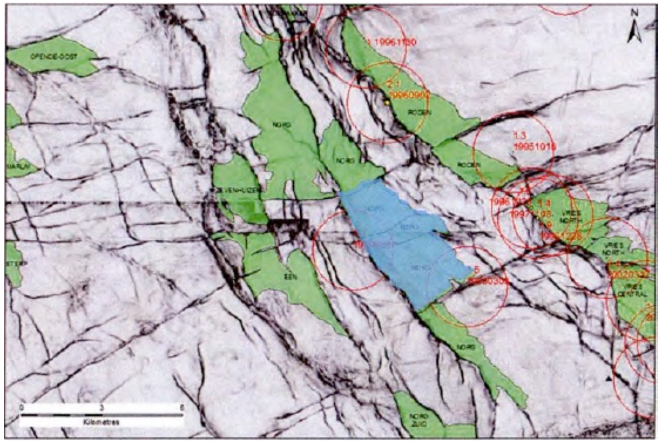

Develop numerical models to simulate the possible inception of fault motion also in «unexpected» configurations

The Netherlands case

Conceptual model

- Schematic geometry representative of the typical configuration of Ducth UGS fields:
  - Independent blocks with different pressure variations
  - Bounding vertical and sub-vertical faults
  - Viscous salt formations on top of the reservoir

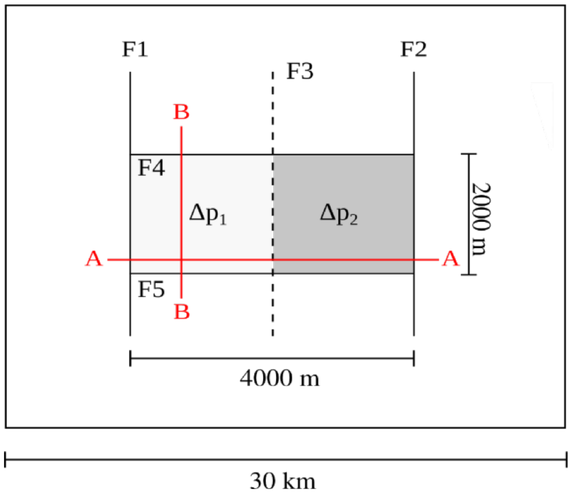

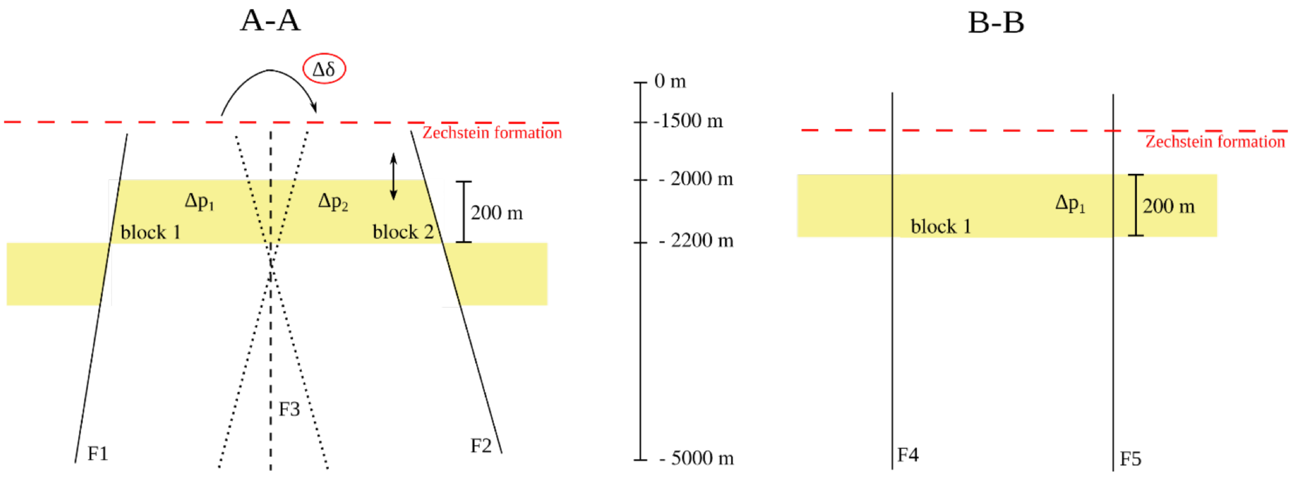

The Netherlands case

Conceptual model

- Geomechanical parameters typical of Dutch UGS formations
- Almost isotropic initial stress state (M_1=0.74, M_2=0.83) with principal directions oriented like the bounding faults

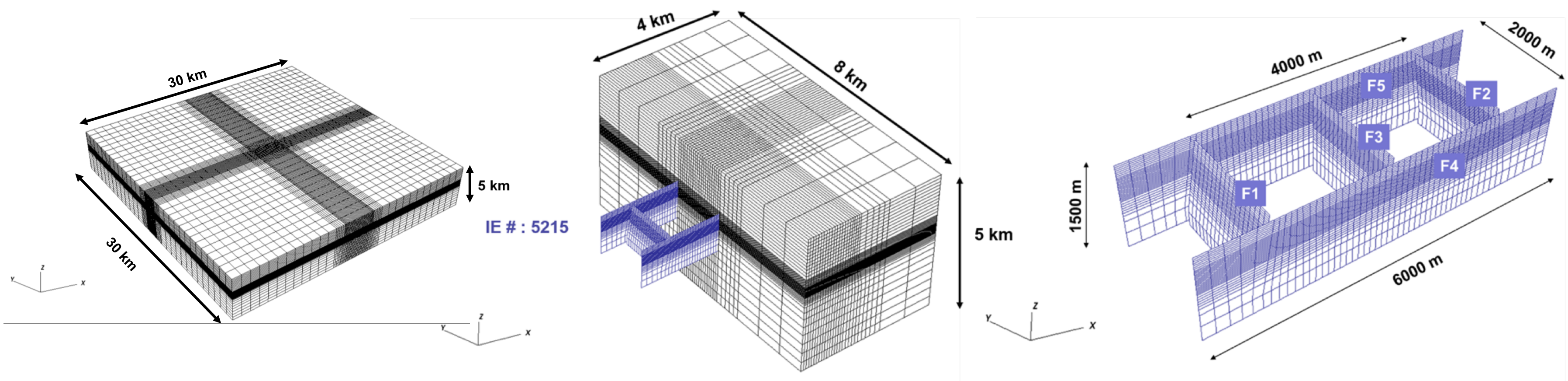

LAYER	DENSITY (kg/m³)	YOUNG MODULUS (GPa)	POISSON RATIO
Overburden	2200	10.0	0.25
Zechstein Salt	2100	40.0	0.3
Reservoir (Upper Rotliegend)	2400	11.0	0.15
Underburden	2600	30	0.2

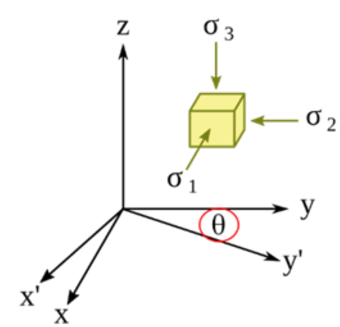

Initial stress regime:

$\sigma_h = \sigma_1 = M_1 * \sigma_3$

$\sigma_H = \sigma_2 = M_2 * \sigma_3$

$\sigma_v = \sigma_3$

Mathematical and numerical model

Quasi-static equilibrium of faults

- Modeling fault/fracture mechanics involves a number of numerical open issues
- Available numerical approaches:

1. Continuous Finite Elements with a different rheology, e.g. [Rutqvist et al. 2008]
   - Ease of implementation
   - Inability to describe slippage and opening
2. Interface frictional elements by penalties, e.g. [Beer, 1985; Cescotto & Charlier, 1993; Juanes et al., 2002; Ferronato et al., 2008]
   - Definiteness preservation, controlled number of DoFs
   - Ill-conditioning, instability, non-linear convergence difficulties
3. Lagrange multipliers, e.g. [Aagaard et al., 2013; Jha & Juanes, 2014; Franceschini et al. 2016]
   - Mathematically robust prescription of constraints
   - Increase of DoFs, saddle-point problem

Mathematical and numerical model

Quasi-static equilibrium of faults

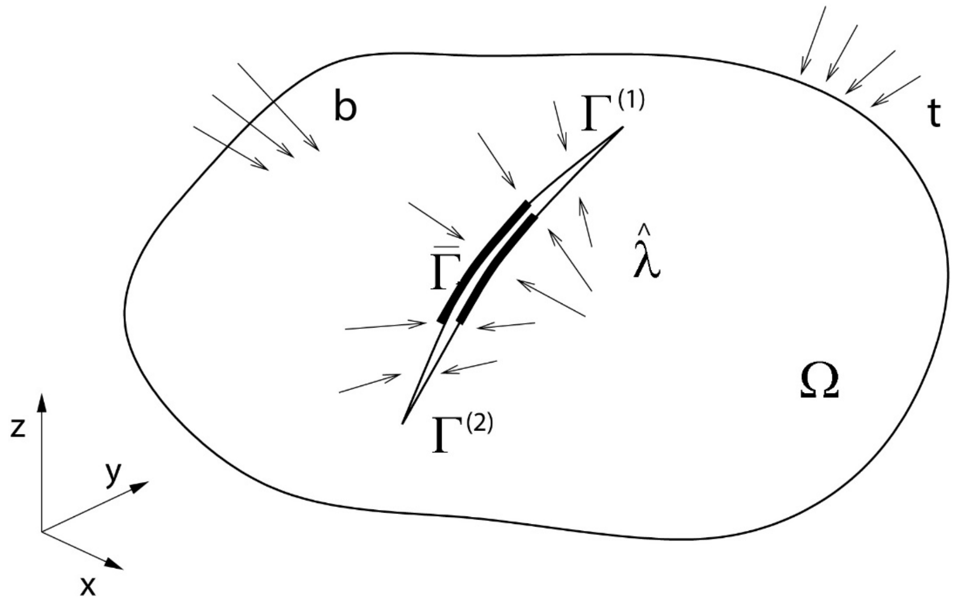

- A fracture is a discontinuity within a 3D porous body made of a pair of friction surfaces in contact each other
- The surfaces can't penetrate and continuity is preserved if:

$$\tau_s \leq \tau_L = c - \sigma_n \tan\varphi, \qquad \sigma_n < 0$$

- The Mohr-Coulomb criterion defines τ_L, but gives no indication as to the direction of the limiting shear vector $\mathbf{t}_L$
- According to the Principle of Maximum Plastic Dissipation, $\mathbf{t}_L$ is such that the friction work W_f is maximum, i.e. is parallel to the slip vector $\mathbf{u}_r$

$$\mathbf{t}_L = \tau_L \frac{\mathbf{u}_r}{\|\mathbf{u}_r\|_2}$$

Mathematical and numerical model

Governing equations

- From a mathematical standpoint, the problem requires the solution of a set of governing PDEs:

$\nabla \cdot \boldsymbol{\sigma} - \boldsymbol{b} = 0$	$\forall \boldsymbol{x} \in \Omega \backslash \Gamma_f$	Momentum balance
$\boldsymbol{u} = \bar{\boldsymbol{u}}$	$\forall \boldsymbol{x} \in \Gamma_u$	Boundary displacement
$\boldsymbol{\sigma} \cdot \boldsymbol{n} = \bar{\boldsymbol{t}}$	$\forall \boldsymbol{x} \in \Gamma_\sigma$	Boundary traction
$\boldsymbol{\sigma} \cdot \boldsymbol{n}_f^- = \boldsymbol{\sigma} \cdot \boldsymbol{n}_f^+ = \boldsymbol{t}$	$\forall \boldsymbol{x} \in \Gamma_f$	Traction continuity

subject to normal contact conditions along Γ_f:

$$t_N = \boldsymbol{t} \cdot \boldsymbol{n}_f \leq 0, \qquad g_N = [\![\boldsymbol{u}]\!] \cdot \boldsymbol{n}_f \geq 0, \qquad t_N g_N = 0$$

and Coulomb frictional contact conditions along Γ_f:

$$\Phi = \|\boldsymbol{t}_T\|_2 - (c - t_N \tan\varphi) \leq 0, \qquad \dot{\boldsymbol{g}}_T - \alpha \frac{\boldsymbol{t}_T}{\|\boldsymbol{t}_T\|_2} = 0,$$

$$\alpha \geq 0, \qquad \Phi\alpha = 0$$

Mathematical and numerical model

Variational formulation

- The discretization is obtained with a mixed finite element approach where displacement **u** and traction **t** on the fault are the main unknowns
- Find $\{\boldsymbol{u}, \boldsymbol{t}\} \in \boldsymbol{\mathcal{S}}_{\boldsymbol{u}}(\Omega) \times \boldsymbol{\mathcal{S}}_{\boldsymbol{t}}(\Gamma_f)$ such that for all $\{\boldsymbol{v}, \boldsymbol{\mu}\} \in \boldsymbol{\mathcal{V}}_{\boldsymbol{u}}(\Omega) \times \boldsymbol{\mathcal{V}}_{\boldsymbol{t}}(\Gamma_f)$

$$\int_{\Omega \setminus \Gamma_f} \nabla^s \boldsymbol{v} : \boldsymbol{\sigma} \, d\Omega - \int_{\Omega \setminus \Gamma_f} \boldsymbol{v} \cdot \boldsymbol{b} \, d\Omega - \int_{\Gamma_\sigma} \boldsymbol{v} \cdot \bar{\boldsymbol{t}} \, d\Gamma + \int_{\Gamma_f} [\![\boldsymbol{v}]\!] \cdot \boldsymbol{t} \, d\Gamma = \boldsymbol{0}$$

$$\int_{\Gamma_f} \boldsymbol{\mu} \cdot [\![\boldsymbol{u}]\!] \, d\Gamma = 0$$

- Introducing as usual the discrete finite element spaces we obtain:

$$\int_{\Omega \setminus \Gamma_f} \nabla^s \boldsymbol{N}_{\boldsymbol{u}} : \boldsymbol{\sigma}^h \, d\Omega + \int_{\Gamma_f} [\![\boldsymbol{N}_{\boldsymbol{u}}]\!] \cdot \boldsymbol{t}^h \, d\Gamma = \boldsymbol{f}$$

$$\int_{\Gamma_f} \boldsymbol{N}_{\boldsymbol{t}} \cdot [\![\boldsymbol{u}^h]\!] \, d\Gamma = 0$$

Mathematical and numerical model

Variational formulation

- The integrals along the fractures Γ_f are computed as the sum of the contributions arising from the portions operating in the «stick» and «slip» modes

$$\int_{\Gamma_f^{st}} [\![\boldsymbol{N_u}]\!] \cdot \boldsymbol{t}^h \, d\Gamma + \int_{\Gamma_f^{sl}} [\![\boldsymbol{N_u}]\!] \cdot (\boldsymbol{n}_f \otimes \boldsymbol{n}_f) \cdot \boldsymbol{t}^h \, d\Gamma + \int_{\Gamma_f^{sl}} [\![\boldsymbol{N_u}]\!] \cdot \boldsymbol{t}_T^{*,h} \, d\Gamma$$

$$\int_{\Gamma_f^{st}} \boldsymbol{N_t} \cdot [\![\boldsymbol{u}^h]\!] \, d\Gamma + \int_{\Gamma_f^{sl}} \boldsymbol{N_t} \cdot (\boldsymbol{n}_f \otimes \boldsymbol{n}_f) \cdot [\![\boldsymbol{u}^h]\!] \, d\Gamma$$

- The problem is highly non-linear because also the «stick» and «slip» portions of the fracture are unknown
- The non-linear problem is finally addressed by a Newton-Raphson scheme

Mathematical and numerical model

Constitutive relationships

- A weakening model is implemented to account for the variation of the friction angle from static to dynamic conditions at the fault slipping:

$$\varphi = \varphi_s + \frac{\varphi_d - \varphi_s}{d_c} \|\boldsymbol{g}_T\|_2, \qquad \|\boldsymbol{g}_T\|_2 \leq d_c$$

$$\varphi = \varphi_d, \qquad \|\boldsymbol{g}_T\|_2 > d_c$$

- A Maxwell model is used to simulate the viscous behaviour of the top salt Zechstein formation:

$$\dot{\boldsymbol{\varepsilon}}_v = V(\mu)\boldsymbol{\sigma}, \qquad \mu = 10^{17}\ Pa \cdot s$$

- The faults are partially sealing and are characterized by an inner pressure variation p_f

Mathematical and numerical model

Discrete problem

- The discrete Jacobian is a large, sparse matrix with a generalized saddle-point structure:

$$J(\boldsymbol{u},\boldsymbol{t}) = \begin{bmatrix} K(\boldsymbol{u}) + E(\boldsymbol{u},\boldsymbol{t}) & C - F(\boldsymbol{u},\boldsymbol{t}) \\ C^T & 0 \end{bmatrix}$$

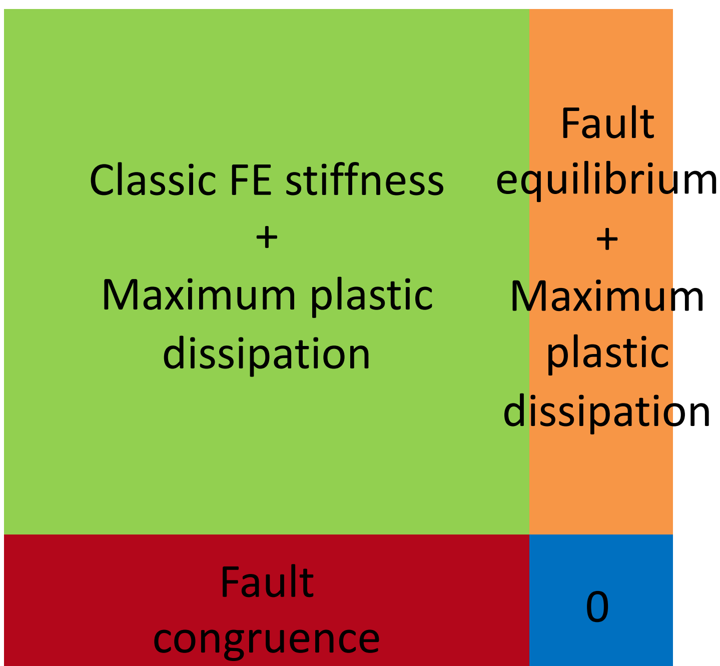

$$K = \int_\Omega \nabla^s \boldsymbol{N}_{\boldsymbol{u}} : \frac{\partial \boldsymbol{\sigma}}{\partial \boldsymbol{\epsilon}} : \nabla^s \boldsymbol{N}_{\boldsymbol{u}} \, d\Omega$$

$$E = \int_{\Gamma_f^{sl}} [\![\boldsymbol{N}_{\boldsymbol{u}}]\!] \cdot \frac{\partial \boldsymbol{t}_T^*}{\partial \boldsymbol{u}} \cdot [\![\boldsymbol{N}_{\boldsymbol{u}}]\!] \, d\Gamma$$

$$C = \int_{\Gamma_f^{st}} [\![\boldsymbol{N}_{\boldsymbol{u}}]\!] \cdot \boldsymbol{N}_{\boldsymbol{t}} \, d\Gamma + \int_{\Gamma_f^{sl}} [\![\boldsymbol{N}_{\boldsymbol{u}}]\!] \cdot (\boldsymbol{n}_f \otimes \boldsymbol{n}_f) \cdot \boldsymbol{N}_{\boldsymbol{t}} \, d\Gamma$$

$$F = \int_{\Gamma_f^{sl}} [\![\boldsymbol{N}_{\boldsymbol{u}}]\!] \cdot \frac{\partial \boldsymbol{t}_T^*}{\partial \boldsymbol{u}} \cdot \boldsymbol{N}_{\boldsymbol{t}} \, d\Gamma$$

Numerical results

Basic activation mechanisms

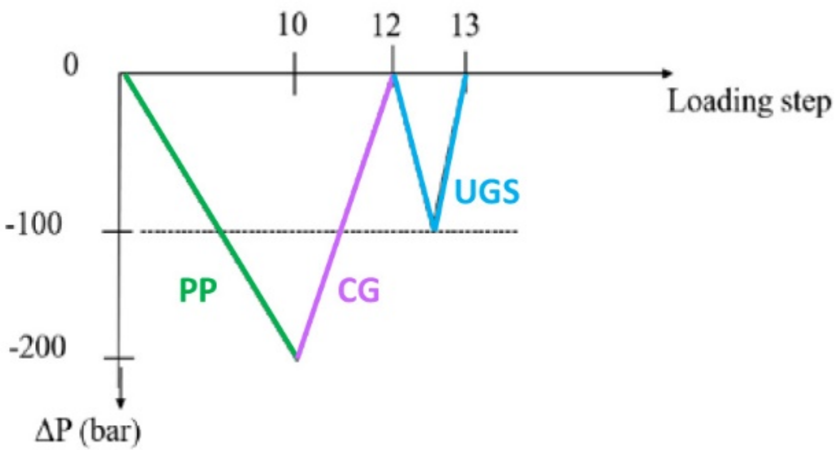

- Pressure history prescribed in the UGS field
- A loading step corresponds to a 1-year time interval
- Critical index:

$$\chi = \frac{\|\boldsymbol{t}_T\|_2}{\|\boldsymbol{t}_T^*\|_2} \leq 1$$

- Sensitivity analysis on different configuration parameters:
  - Block offset (0-200 m)
  - Central fault dip (-25° - 25°)
  - Reservoir and caprock stiffness
  - Fault properties
  - Biot coefficient (0.6 – 1.0)
  - Initial stress regime (M_1=M_2=0.4)
  - Pressure variation (0-200 bar)
  - Fault pressure (0-200 bar)

Numerical results

Basic activation mechanisms

Primary Production

Primary Production

Cushion Gas

Gas Storage

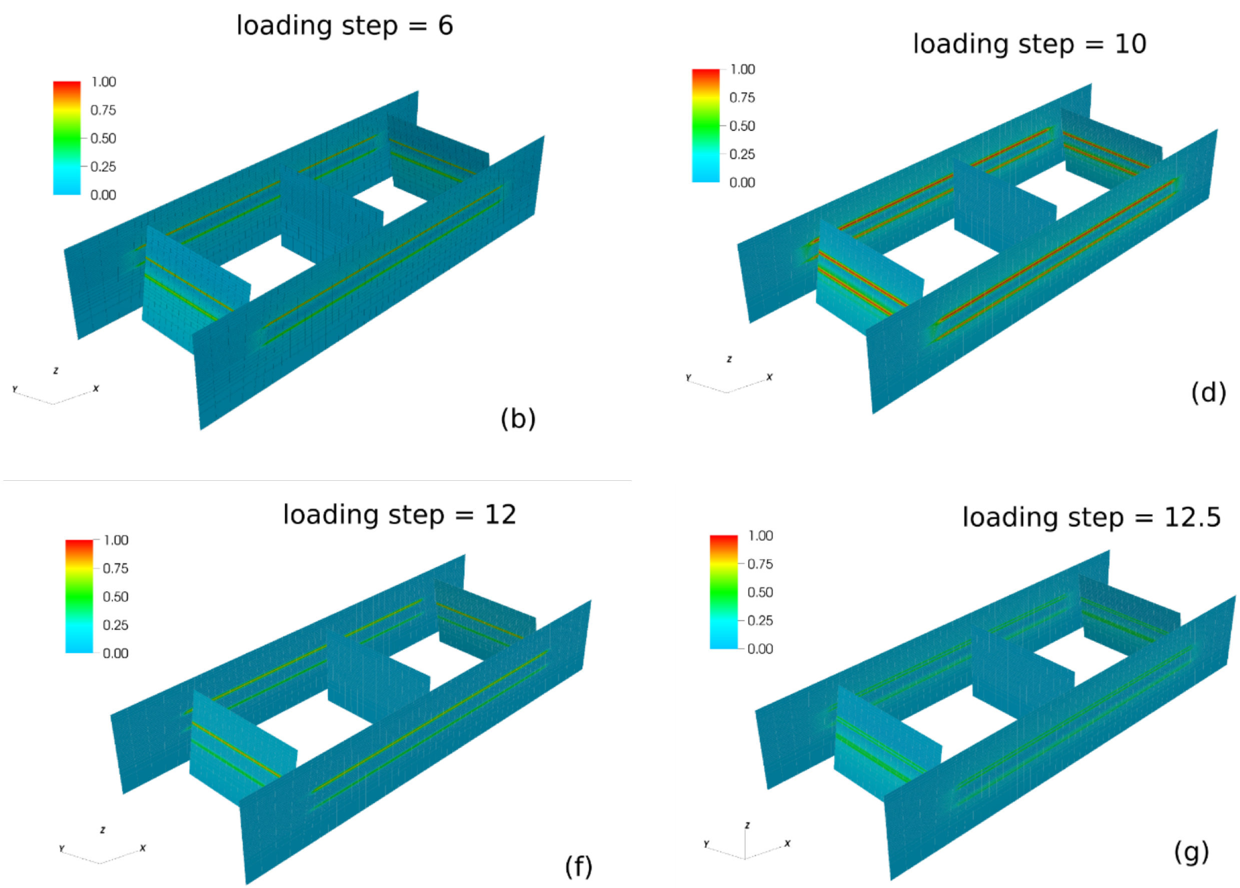

Numerical results

Basic activation mechanisms

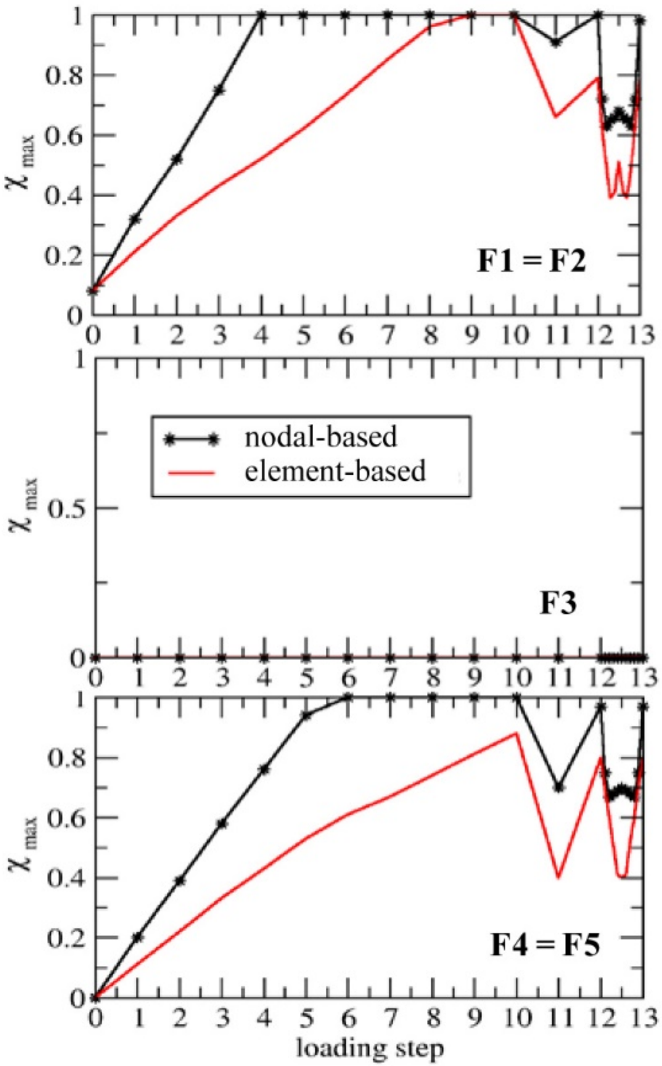

- Critical index on the bounding faults vs the loading steps

- Fault thickness with χ>0.8

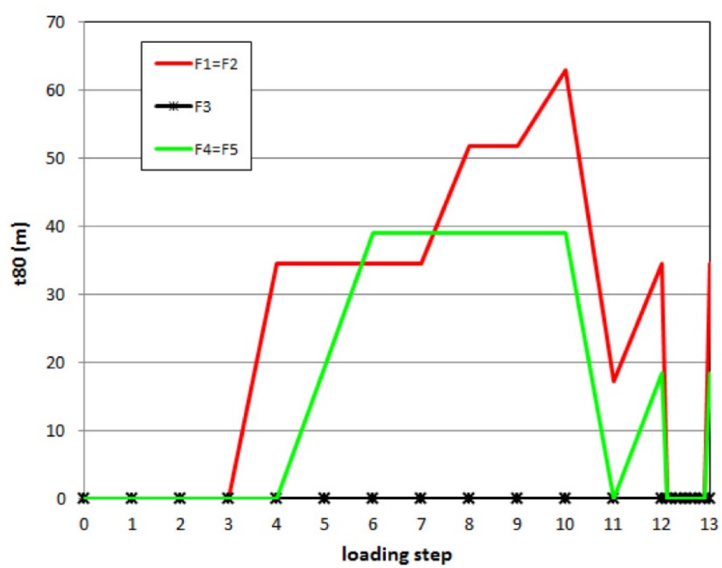

Numerical results

Basic activation mechanisms

- Stress on a bounding fault during Primary Production, Cushion Gas e Gas Storage

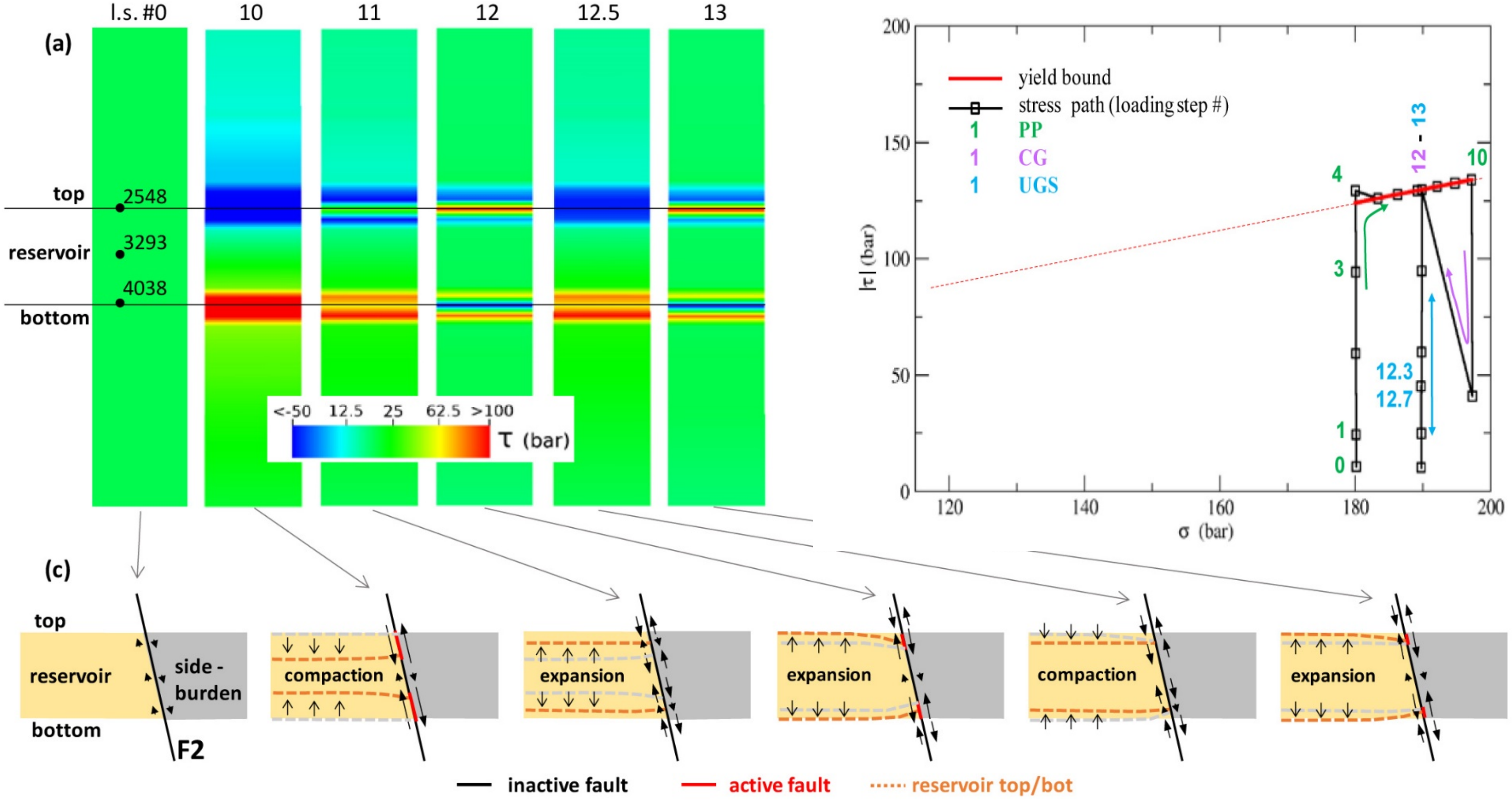

Numerical results

Sensitivity analysis results

- Modifying the mechanical and geometrical properties can anticipate or delay the fault activation, or increase the amount of slippage and the activated area

  - the initial stress regime can play a major role: decreasing significantly the horizontal principal components favors an early fault reactivation, with a large area critically stressed and significant sliding
  - factors increasing the activation risk: (1) a reduced friction angle; (2) an offset between producing blocks; (3) stiffness contrasts between reservoir, caprock, sideburden, and underburden; (4) uneven pressure change in adjacent compartments
  - most critical configuration: 200-m compartment offset, a relatively small friction angle, and a viscous caprock

Conclusions…

- A 3D modeling study has been developed on a conceptual configuration representative of the Dutch UGS fields to evaluate how and when faults bounding a compartmentalized reservoir can be reactivated during the UGS activities
- The fault mechanics is simulated with the aid of a Lagrangian formulation with a non-linear weakening behavior for the friction angle, a viscous salt caprock and partially sealing faults
- The investigation has been carried out in detail on a reference benchmark and by changing mechanical and geometrical configurations in an extensive sensitivity analysis

Università degli Studi di Padova

… and preliminary practical indications

- Fault reactivation may occur “unexpectedly” during Cushion Gas and Underground Gas Storage stages, following more expected reactivations during Primary Production
- Activation during Primary Production leads to a stress redistribution and a new "equilibrated" configuration that is re-loaded, in the opposite direction, when the pressure variation changes the sign at the Cushion Gas injection
- The settings more prone to activation during Primary Production are also the most critical ones during Cashion Gas injection and Underground Gas Storage

- A preliminary indication may rely on <u>limiting the pressure recovery</u> during the storage operations <u>if a reactivation has been already experienced during the Primary Production</u>

UNIVERSITÀ DEGLI STUDI DI PADOVA

Dept. of Civil, Environmental and Architectural Engineering

Thank you for your attention

SIAM Conference on Mathematical and Computational Issues in the Geosciences (GS19)

March 11-14, 2019 – Houston, TX

Linear solver

Preconditioning

- Solving a linear problem with a saddle-point matrix is a common issue in several applications, e.g., flow problems in mixed form, coupled consolidation, Navier-Stokes equations, etc.
- The most effective approach proceeds as follows:
  - Solve for the incremental displacements $\delta\mathbf{u}$ in the first equation

$$\delta\mathbf{u} = (K+E)^{-1}\left[\mathbf{f} - (C-F)\delta\boldsymbol{\lambda}\right]$$

  - Replace $\delta\mathbf{u}$ in the second equation and solve for $\delta\lambda$

$$\delta\boldsymbol{\lambda} = \left[C^T (K+E)^{-1}(C-F)\right]^{-1} C^T (K+E)^{-1}\mathbf{f}$$

  - Approximate the application of the inverse of 1,1 block (K+E) and the Schur complement S:

$$S = C^T (K+E)^{-1}(C-F)$$

  - Use these equations to apply a «preconditioner» to J

- Numerical ingredients to define an effective preconditioner for a Krylov subspace solver:
  - Approximation of $(K+E)^{-1}$
  - Approximation of S and of S^{-1}
- Approximating the application of the inverse of $(K+E)$ is not an issue and can be done in several different ways, e.g., Incomplete Factorizations, Sparse Approximate Inverses, Algebraic Multigrid
- The difficulty lies in approximating the Schur complement S and its inverse
- Three approaches:
  - Factored Sparse Approximate Inverse (FSAI)
  - Block Diagonal Schur complement (BDS)
  - Least-Square Commutator (LSC)

Factored Sparse Approximate Inverse (FSAI)

- For the computation of *S* an explicit approximation of $(K+E)^{-1}$ is required
- Since (K+E) is SPD, we can use an adaptive FSAI approximation [Janna et al. 2015]:

$$(K+E)^{-1} \approx GG^T \quad \Rightarrow \quad S \approx C^T GG^T (C-F) \approx H^T H$$

- The inverse of the Schur complement is then applied with a direct solver or another FSAI approximation

Block Diagonal Schur complement (BDS)

- From a physical point of view, $\delta\lambda$ ensures the continuity of the displacement through the fracture
- Such a continuity can be approximately prescribed on a node-by-node basis considering the local stiffness associated to each node only

Linear solver

BDS approach

- From a purely algebraic point of view, this means considering the restrictions $(K+E)^{(k)}$ of $(K+E)$ corresponding to the entries related to DoFs of the elements sharing the k-th node:

$$S \approx \sum_k C^{(k),T} R^{(k),T} K^{(k),-1} R^{(k)} \left(C-F\right)^{(k)} E_k E_k^T$$

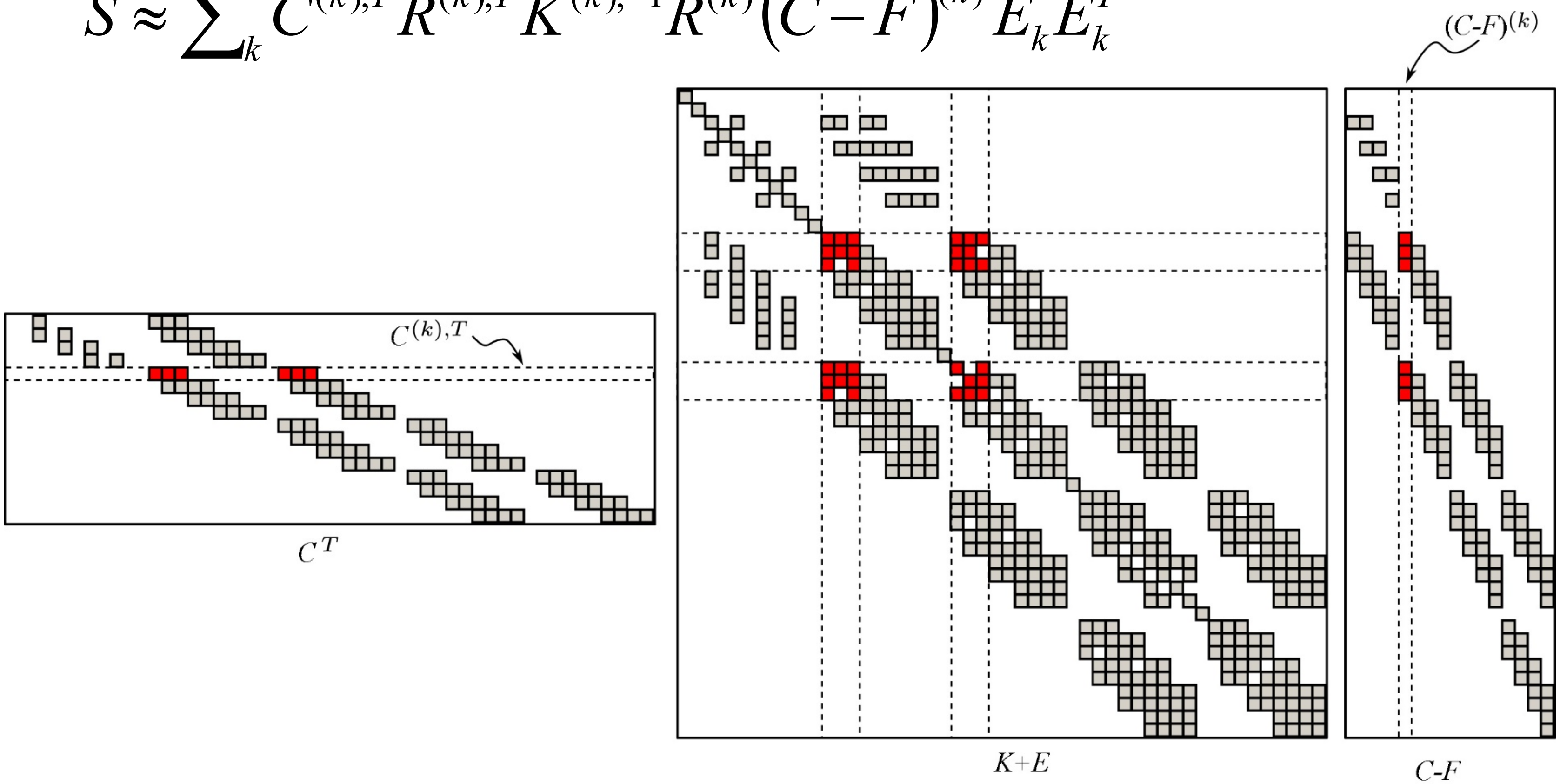

Least-Square Commutator (LSC)

- This approach was originally introduced for Navier-Stokes problems in order to avoid the inversion of the 1,1 block for approximating the inverse of S [Elman et al. 2006]
- The objective is to find a commutator K_p such that:

$$(K+E)C \approx CK_p \quad \Rightarrow \quad K_p = \left(C^T C\right)^{-1} C^T (K+E) C$$

- From the previous approximation it follows also that:

$$CK_p^{-1} \approx (K+E)^{-1} C$$

so the inverse of the Schur complement can be written as:

$$S^{-1} = \left[C^T (K+E)^{-1} (C-F)\right]^{-1} \approx \left[C^T (K+E)^{-1} C\right]^{-1} \approx \left[C^T C K_p^{-1}\right]^{-1} \approx$$

$$\approx K_p \left(C^T C\right)^{-1} = \underline{\left(C^T C\right)^{-1} C^T (K+E) C \left(C^T C\right)^{-1}}$$

Linear solver

LSC approach

- The advantage of the LSC approach is that the inverse of S is directly available using the blocks of J and $(K+E)^{-1}$ is not needed
- In our fault/fracture formulation, $C^T C$ is diagonal, so that the computation and application of its inverse is totally inexpensive
- The final Schur complement inverse can be also seen as:

$$S^{-1} \approx C^{+}\left(K+E\right)^{-1} C^{+,T}$$

where C^+ is the pseudo-inverse of C according to the Moore-Penrose definition

- *Theorem*. The eigenvalues λ of $S^{-1}S$, where S^{-1} is approximated by the LSC, are bounded from below by 1:

$$1 \leq \lambda \leq 1 + \left\|P\right\|^2 \left\|H\right\|$$

with P and H matrices that depend on the SVD decomposition of C and on K

Università degli Studi di Padova

Numerical results

Test case

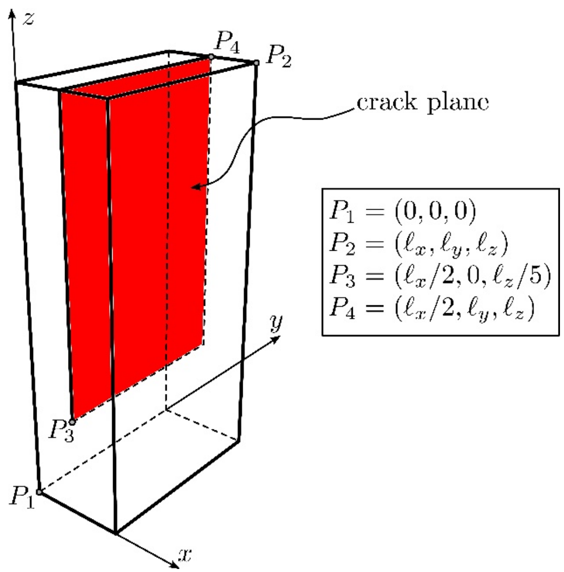

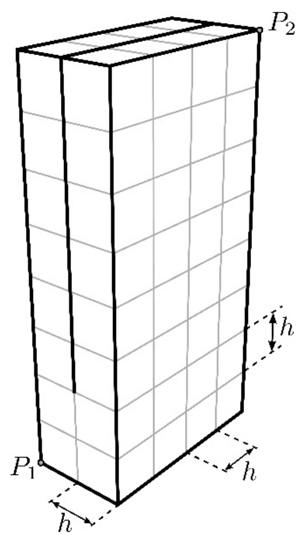

h	# u dofs	# λ dofs
l/2	615	120
l/4	3,267	432
l/8	20,451	1,632
l/16	142,659	6,336
l/32	1,060,995	24,960

Iteration count to converge vs. the mesh size

l/h	FSAI(5,.01)	FSAI(20,.01)	BDS	LSC
2	22	20	27	22
4	29	25	34	27
8	35	20	40	32
16	42	36	48	39
32	49	43	56	46

Numerical results

Test case

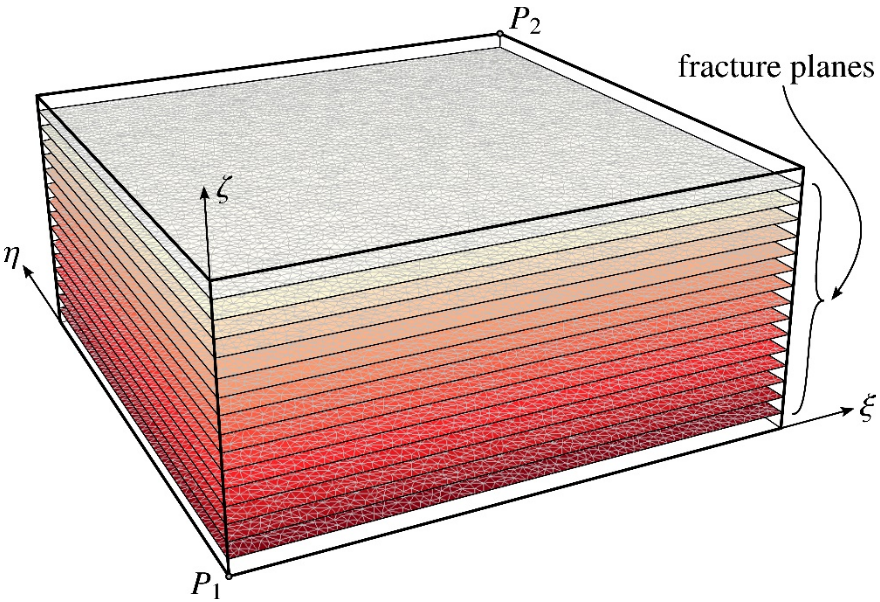

Multiple fractured elastic medium with 15 discontinuities

# u dofs	# λ dofs	Ratio
379,983	167,799	0.442

	FSAI + DIR		FSAI + FSAI		BDS		LSC	
$(K+E)^{-1}$	# iter	Time [s]	# iter	Time [s]	# iter	Time [s]	# iter	Time [s]
FSAI	409	96.5	428	80.7	***482***	***68.1***	866	161.6
IC	229	73.5	***227***	***67.9***	574	80.6	407	77.8
exact	100	--	92	--	268	--	99	--

Numerical results

Real-world applications

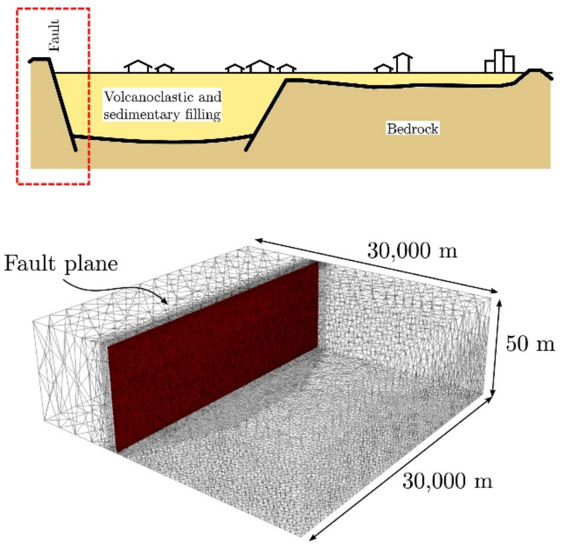

A - Mexico

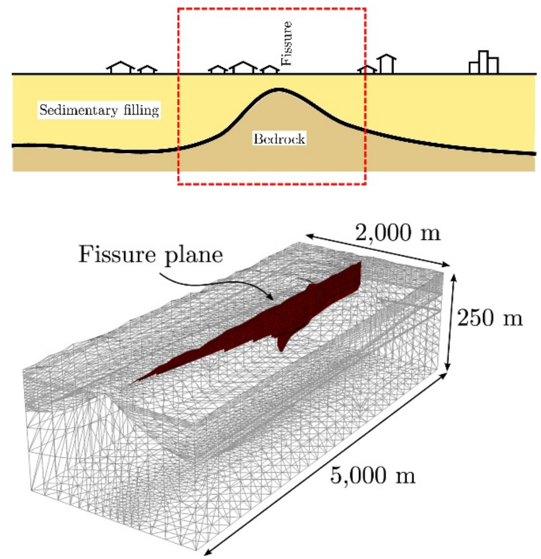

B - China

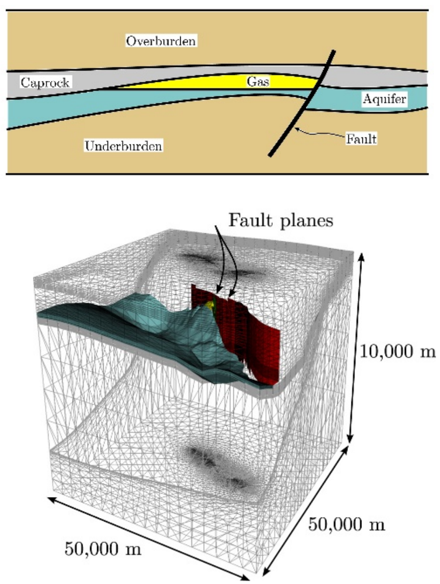

C - Italy

	# u dofs	# λ dofs	# tot dofs	Nnz(K+E)	Nnz(C-F)	Nnz(C^T)
Case A	171,150	12,027	183,177	7,313,814	72,162	72,162
Case B	69,909	2,757	72,666	2,946,915	16,542	16,542
Case C	1,142,655	38,109	1,180,764	49,858,749	228,654	228,654

Numerical results

Real-world applications

A - Mexico

	FSAI + DIR		FSAI + FSAI		BDS		LSC	
$(K+E)^{-1}$	# iter	Time [s]	# iter	Time [s]	# iter	Time [s]	# iter	Time [s]
FSAI	123	9.6	***126***	***9.1***	255	13.0	175	12.3
IC	98	10.3	97	10.1	240	12.2	***59***	***6.8***
exact	35	--	34	--	126	--	23	--

B - China

	FSAI + DIR		FSAI + FSAI		BDS		LSC	
$(K+E)^{-1}$	# iter	Time [s]	# iter	Time [s]	# iter	Time [s]	# iter	Time [s]
FSAI	***72***	***1.7***	73	2.0	371	5.5	77	2.6
IC	34	1.6	34	1.8	189	3.0	***24***	***0.8***
exact	21	--	24	--	129	--	12	--

Numerical results

Real-world applications

C - Italy

$(K+E)^{-1}$	FSAI + DIR # iter	FSAI + DIR Time [s]	FSAI + FSAI # iter	FSAI + FSAI Time [s]	BDS # iter	BDS Time [s]	LSC # iter	LSC Time [s]
FSAI	***496***	***156.5***	623	172.7	--	--	768	287.1
IC	194	116.1	195	128.3	--	--	***125***	***73.2***
exact	50	--	50	--	276	--	35	--